horticulturae

MDPI

Article

Characterization and Expression Analysis of the UDP Glycosyltransferase Family in Pomegranate (*Punica granatum* L.)

Guixiang Li [1,2,†], Jiyu Li [2,3,†], Gaihua Qin [2,3,*], Chunyan Liu [2,3], Xin Liu [1,2], Zhen Cao [2,3], Botao Jia [2,3] and Huping Zhang [1,*]

1 College of Horticulture, Nanjing Agricultural University, Nanjing 210095, China
2 Key Laboratory of Horticultural Crop Genetic Improvement and Eco-Physiology of Anhui Province, Institute of Horticultural Research, Anhui Academy of Agricultural Sciences, Hefei 230031, China
3 Key Laboratory of Germplasm Innovation and Utilization of Horticultural Crop (Co-Construction by Ministry and Province), Ministry of Agriculture and Rural Affairs, Institute of Horticultural Research, Anhui Academy of Agricultural Sciences, Hefei 230031, China
* Correspondence: qghahstu@163.com (G.Q.); hpzhang@njau.edu.cn (H.Z.)
† These authors contributed equally to this work.

Abstract: UDP glycosyltransferases (UGTs) play an indispensable role in regulating signaling pathways and intracellular homeostasis in plants by catalyzing the glycosylation of metabolites. To date, the molecular characteristics and potential biological functions of the *UGT* gene family in pomegranate (*Punica granatum* L.) remain elusive. In this study, a total of 120 *PgUGT* genes were identified in the pomegranate genome. Phylogenetic analysis revealed that these *PgUGT*s were clustered into 15 groups: 13 conserved groups (A–J and L–N) and two newly discovered groups (P and R). Structural analysis showed that most members in the same evolutionary branch shared similar motifs and gene structures. Gene duplication analysis demonstrated that tandem duplication and fragment duplication were the primary driving force for the expansion of the *PgUGT* family. Expression analysis based on RNA-seq data indicated that *PgUGT*s exhibited various expression profiles in different pomegranate tissues. We further analyzed the expression patterns of the *PgUGT*s of groups E and L in the seed coat of the hard-seeded cultivar 'Dabenzi' and the soft-seeded cultivar 'Tunisia' at different developmental stages. There were eight *PgUGT*s with high expression levels in the seed coat of both cultivars: *PgUGTE10* was highly expressed in inner and outer seed coats; *PgUGTE20*, *PgUGTE21*, *PgUGTL6*, *PgUGTL11*, and *PgUGTL12* were mainly expressed in the inner seed coat; and *PgUGTE12* and *PgUGTL13* were mainly expressed in the outer seed coat. Interestingly, the relative expression levels of *PgUGTE10* and *PgUGTL11* in 'Tunisia' were higher than in 'Dabenzi'. In the seedlings, quantitative real-time PCR analysis showed that the expression level of *PgUGTE10* was induced by brassinolide treatment, while the expression of *PgUGTL11* was up-regulated both by indole-3-acetic acid and the brassinolide treatment. In addition, the expressions of *PgUGTE10* and *PgUGTL11* were highly correlated with the expression of genes involved in hormone signaling and lignin biosynthesis pathways. These results suggested that *PgUGTE10* and *PgUGTL11* are potential candidate genes involved in seed hardness development by catalyzing the glycosylation of specific substrates.

Keywords: UDP glycosyltransferases; expression analysis; *Punica granatum* L.; seed coat; hormones; seed hardness development

check for updates

Citation: Li, G.; Li, J.; Qin, G.; Liu, C.; Liu, X.; Cao, Z.; Jia, B.; Zhang, H. Characterization and Expression Analysis of the UDP Glycosyltransferase Family in Pomegranate (*Punica granatum* L.). *Horticulturae* **2023**, *9*, 119. https://doi.org/10.3390/horticulturae9010119

Received: 12 December 2022
Revised: 6 January 2023
Accepted: 9 January 2023
Published: 16 January 2023

1. Introduction

The pomegranate (*Punica granatum* L.) fruit is rich in secondary metabolites, which have significant medicinal and health care functions, and pomegranate has the reputation as a 'super fruit' [1,2]. The edible proportion of the pomegranate fruit depends largely on the size of the seed coat, which is composed of outer and inner seed coats. Due to the

differential accumulation of metabolites during seed coat development, the outer seed coat develops into an expanded fleshy tissue, while the inner seed coat develops into a compressed firm tissue. Seed hardness is an important quality characteristic of fresh fruit, which directly affects the fruit's marketability. Thus, genetic studies of seed hardness development have attracted more attention.

In pomegranates, seed hardness development is a process of lignification of the inner seed coat [3]. Lignin is produced in the cell wall by the oxidative coupling of monolignols that are synthesized in the cytoplasm via the phenylpropanoid pathway [4]. The glycosylation of monolignols is essential for their activity and transport to the cell wall for polymerization or to the vacuole for storage [5,6]. Therefore, monolignol glycosylation plays an important role in the regulation of lignin biosynthesis.

Previous studies showed that seed coat development is regulated by auxin exported from the endosperm [7–9]. Auxin regulates most physiological processes through signal transduction, including lignin biosynthesis [10–12]. Much work has been conducted to clarify the molecular mechanisms underlying the auxin-mediated signaling pathway that regulates lignin formation. In pomegranates, cell divisions in the early seed coat development stage and lignin accumulation in the later seed coat development stage limit the seed hardness. A lack or excess of auxin is unfavorable to plant growth and development [13]. Brassinolide (BR) has been shown to play a regulatory role in the development of the secondary xylem of *Liriodendron tulipifera* [14]. The lignin content in peach fruit was increased by BR treatment [15]. In *Arabidopsis*, BR may participate in signal transduction in cell wall deposition [16]. Both IAA and BR play decisive roles in the pattern of the vascular bundle formation cycle of buds [17], and BR can also induce the formation of lignin in suspension cells [18,19]. Glycosylation is one of the mechanisms maintaining cellular hormone homeostasis through the regulation of the level of biological activity and subcellular distribution of the glycosylated hormone [20]. Therefore, hormone homeostasis mediated by glycosylation may play an important role in regulating seed hardness development.

The Family-1 UDP glycosyltransferases (UGTs) comprise a multigene family in higher plants. The UGTs play an indispensable role in plant growth and development by catalyzing the glycosylation of small molecule compounds with a wide range of substrates, including lipophilic receptors, hormones, and secondary metabolites [21,22]. Some plant UGTs were isolated and functionally characterized. In *Arabidopsis thaliana*, 112 *UGTs* were identified and divided into 14 phylogenetic groups (A–N) based on amino acid sequence homology [23]. In addition, several new phylogenetic groups (groups R [24], Q [25], O, and P [26]) were found in other higher plants, indicating that some variation in *UGTs* occurred in different plants. In previous studies, AtUGT72E1–3 was first proven to be glycosylate lignin precursors [27,28]. The knockout of *UGT72E2* in *Arabidopsis* can significantly reduce the content of coniferyl alcohol and sinapyl alcohol in roots and leaves [29]. Recombinant UGT72B1 protein has a higher catalytic activity for coniferyl alcohol and coniferyl aldehyde in vitro, with the *UGT72B1* mutant plant showing intensified ectopic lignification of flower stems [30]. Recent studies showed that PbUGT72AJ2 affects the stone cell development of pear fruit through glycosylated coniferol and sinapinol [31]. The first indole-3-acetic acid (IAA) glycosyltransferase found in corn was IAGLU, which catalyzes IAA to produce indoleacetyl sugar ester [32]. In *Arabidopsis*, UGT84B1 was shown to glycosylate IAA to form the corresponding sugar ester, and *UGT84B1* overexpression resulted in a series of auxin-deficient phenotypes [33,34]. The gene *UGT74E2* regulates plant morphogenesis and responses to drought and salt stress through glycosylated indole-3-butyric acid (IBA) [35]. The analysis of biochemical characteristics in vitro showed that UGT74D1 was able to glycosylate IAA, indole-3-propionic acid, and naphthene acid in addition to preferentially glycosylating IBA [36]. *UGT73C5* and *UGT73C6* play important roles in regulating BR homeostasis in *Arabidopsis* [37,38]. These results indicate that the glycosylation modification of hormones plays an important role in plant growth and development. At present, only a few pomegranate *UGT* genes are identified and functionally characterized. Previously, PgUGT84A23 (PgUGTL13 in this study) and PgUGT84A24 (PgUGTL12 in this study)

were shown to catalyze gallic acid and UDP-glucose to form β-glucogallin (galloylglucose ester) [39]. PgUGT95B2 (PgUGTR2 in this study) prefers flavones and flavonols as substrates in enzyme activity [40]. However, the other *PgUGT*s remain to be identified.

In this study, we presented genome-wide identification and classification of *UGT* family members in pomegranates and described their evolution and expansion. *UGT* gene expression profiles in pomegranate tissues and seed coats at different development stages were examined to study their potential function in pomegranate, and stimulus-induced expression patterns of selected *UGT* genes were investigated under IAA and BR treatment. This study could provide useful theoretical support for functionally characterizing and understanding the role of pomegranate *UGT* genes.

2. Materials and Methods

2.1. Plant Materials and Treatments

Pomegranate cultivar 'Dabenzi' were collected from Hefei City, Anhui Province in China. For gene expression analysis under hormones treatments, the seeds of 'Dabenzi' were sown in soil and moved to half-strength Hoagland nutrient solution with growth conditions of temperature 25 °C, relative humidity 60%, and photoperiod 16 h/day after the seedlings grew four leaves. When the seedlings reached a height of about 10 cm, they were treated with 0.5 mM IAA for 6 or 12 h [41] or 1 μM BR for 3 and 5 days [42]. At the corresponding time points, pomegranate root tissue was harvested.

2.2. Identification of Pomegranate UGT Gene Family

The whole genome and protein sequences of 'Dabenzi' were used in this study [43]. The *Arabidopsis* UGT protein sequences were downloaded from the CAZy-GT1 website (http://www.cazy.org/GT1.html; accessed on 2 May 2022) as reference sequences, and the conserved PSPG domain was obtained from the Pfam website (http://pfam.xfam.org/; accessd on 3 May 2022). First, the PSPG domain was used as a query sequence to Blastp search the pomegranate protein genome database with Biological Sequence Alignment Editor (BioEdit) software, with E value set at 1×10^{-5}, and obtain the candidate sequences. Multi-sequence alignment was then performed with DNAMAN software, and any sequences without the conserved sequence of the PSPG domain were deleted. Finally, the CDD (https://www.ncbi.nlm.nih.gov/Structure/bwrpsb/bwrpsb.cgi; accessed on 21 May 2022) and SMART (http://smart.embl.de; accessed on 2 June 2022) databases were used to further verify the candidate genes, removing members without conserved domains or with incomplete domains [44,45]. The ProtParam tool (http://web.expasy.org/protparam/; accessed on 15 June 2022) was used for predicting the molecular weight (MW) and isoelectric point (pI) of PgUGTs.

2.3. Phylogenetic Analysis of PgUGTs

The *PgUGT*s were aligned with 112 *AtUGTs* to construct a phylogenetic tree by the neighbor-joining method using MEGA10.2.2 software. The bootstrap values were calculated with 1000 replications, and other parameters were defaulted. The *PgUGTs* were classified and named according to Cui et al. [24] and Li et al. [46].

2.4. Gene Structure and Conservative Motif Analysis of PgUGTs

The conserved motifs of the *PgUGT* family were identified using the MEME website (http://meme.nbcr.net/meme/cgi-bin/meme.cgi; accessed on 1 June 2022), with the maximum number of motifs as 20 [47]. The exon–intron structures of the *PgUGT*s were determined through comparison of the coding sequence of each *PgUGT* with its genomic sequence using TBtools software [48]. The amino acid composition of the PSPG-box of 120 *PgUGT*s was analyzed using the SeqLogo function in TBtools [49].

2.5. Chromosomal Locations and Gene Duplication of PgUGTs

The specific chromosomal location of each *PgUGT* was obtained from the pomegranate genome database and visualized using the Gene Location Visualize from GTF/GFF function in TBtools. Two or more adjacent genes within a region of 200 kb located on a chromosome were defined as tandem duplications, while homologous genes located on a single chromosome or different chromosomes were defined as transposition/segmental duplications [50]. The intra-species collinearity analysis was performed using the Synteny Visualization function in TBtools. For each duplication gene pair, the Ka (nonsynonymous substitution rate) and Ks (synonymous substitution rate) were calculated through the TBtools simple Ka/Ks calculator program [51].

2.6. Cis-Regulatory Element Analysis of PgUGTs

The upstream 2000-bp sequences of *PgUGT*s were extracted as the promoter sequences using TBtools, and *cis*-regulatory elements (CREs) in the promoter sequences were predicted using the PlantCARE online website (http://bioinformatics.psb.ugent.be/webtools/plantcare/html; accessed on 4 June 2022) [52].

2.7. Expression Pattern Analysis of PgUGTs

The abundance of *PgUGT* transcripts in different tissues of 'Dabenzi' and in inner and outer seed coats of hard-seeded cultivar 'Dabenzi' and soft-seeded cultivar 'Tunisia' were collected from the NCBI Sequence Read Archive database (accession numbers SRP100581 and SRP212814) [43,53]. The transcriptional abundances of *PgUGT*s were estimated using the fragments per kilobase per million (FPKM) method and illustrated with a heat map generated by TBtools [48].

2.8. Quantitative Real-Time PCR (qRT-PCR) Analysis

Total RNA was extracted from the samples using the RNAprep Pure Plant Kit (polysaccharide and polyphenolic-rich) (TianGen Bio-chemical Technology Co., Ltd., Beijing, China). The cDNA synthesis was carried out using a Prime ScriptTM RT Reagent Kit (TaKaRa Biomedical Technology Co., Ltd., Tokyo, Japan).

The qRT-PCR was carried out using SYBR Premix Ex Taq II Kit (TaKaRa). A melt curve analysis was used to verify that the primer dimer had not been quantified. *PgACTIN7* was used as a reference gene. Relative expressions of genes were compared using the $2^{-\Delta\Delta Ct}$ method. The primers were designed using Primer Premier 5 software and were listed in Table S1. The histogram was constructed using Prism software [54].

2.9. Co-Expression Analysis

The transcriptome data were obtained from the RNA-seq data (accession number SRP100581). Firstly, genes with expression in the seed coat were selected for Kyoto Encyclopedia of Genes and Genomes (KEGG) analysis. Then, genes enriched in phenylpropanoid biosynthesis and hormone signaling pathways were used to construct co-expression analysis with the candidate *PgUGT*s using Pearson's correlation coefficient (PCC). The detected associations with PCC > 0.99 were selected. Networks were visualized using Cytoscape v3.7.1 [55].

2.10. Subcellular Localization of PgUGTL11 and PgUGTE10

To investigate the subcellular localization of PgUGTL11 and PgUGTE10, we constructed *35S::PgUGTL11/PgUGTE10–GFP* fusion vectors and transformed them into tobacco epidermal cells. The pCAMBIA1305–GFP empty vector was used as the control. After 2–3 days of incubation, the localization of these proteins was observed under a laser confocal microscope (LSM 800, Zeiss, Jena, Germany).

3. Results

3.1. Identification and Phylogenetic Analysis of PgUGTs

A total of 120 *PgUGT*s were identified in the pomegranate genome. The *PgUGTs* encoded proteins of 245 (PgUGTA2) to 1364 aa (PgUGTE22), with an MW range of 27.3–151.2 kDa. The predicted pI of PgUGTs was 4.79 (PgUGTL11) to 8.70 (PgUGTE6) (Table S2).

The phylogenetic tree of 120 *PgUGT*s and 112 *AtUGT*s showed that *PgUGT*s were distributed in 15 groups (A–J, L–N, P, and R) (Figure 1), including two newly discovered groups (P and R), which do not exist in *Arabidopsis* but are present in some plants such as apple and tea (Figure S1) [24,56]. Group E is the largest *UGT* subfamily (23 genes), while group N is the smallest (only one gene). Compared with *Arabidopsis*, group G had a significant increase in numbers, while groups K, O, and Q showed a loss of *PgUGT*s.

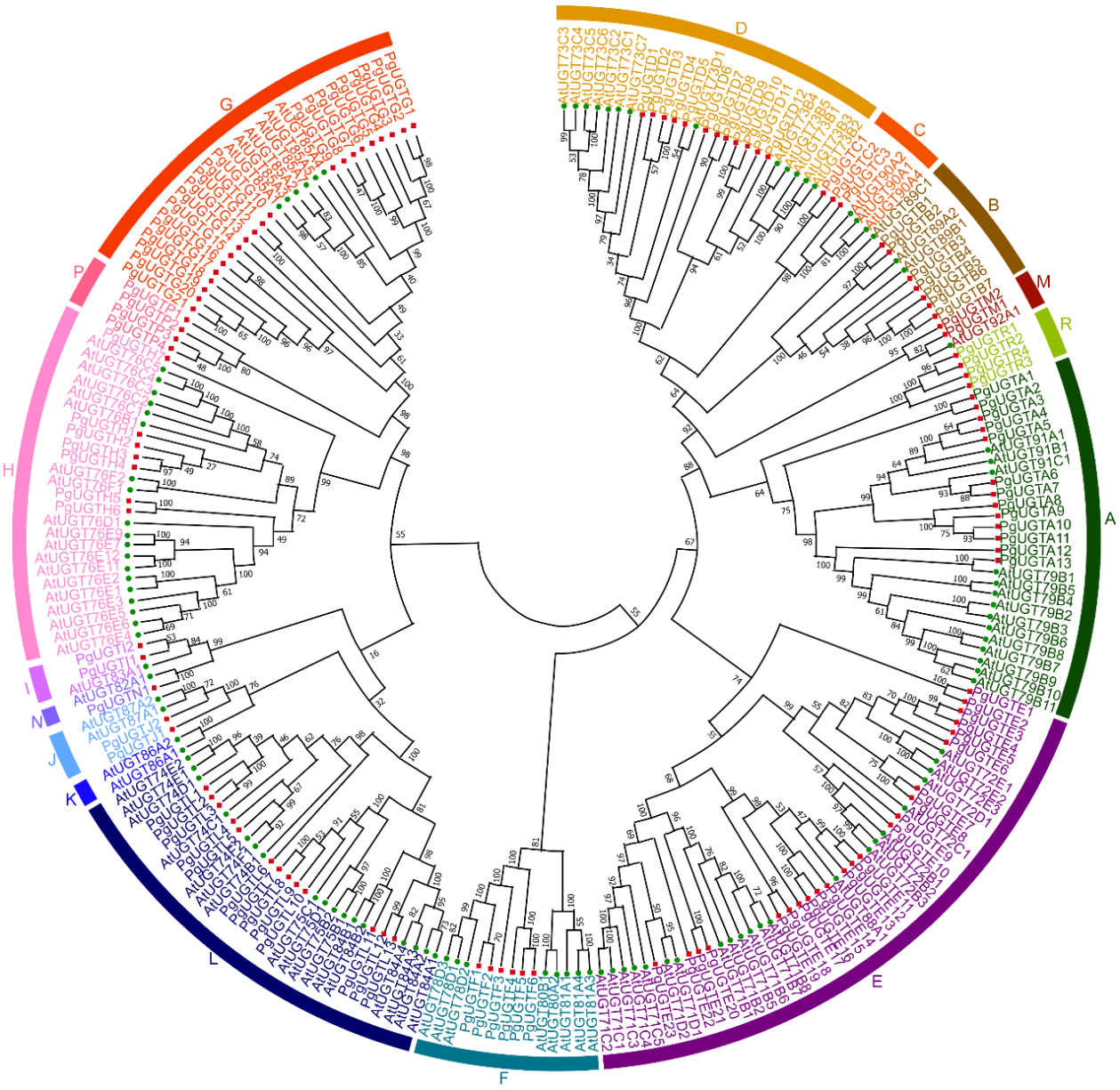

Figure 1. Phylogenetic analysis of UGT proteins in pomegranate and *Arabidopsis*. The capital letters (A–J, L–N, P, and R) represent different groups. The phylogenetic tree was generated by the neighbor-joining method using MEGA 10 software with 1000 bootstrap replicates.

3.2. Conserved Motifs and Gene Structure Analysis of PgUGTs

The conserved motifs and gene structure were analyzed to further explore the evolutionary relationship between different PgUGTs. The results showed that the number of motifs of *PgUGT* family members ranged from 9 to 19, and all members contained motif 1 (PSPG-box) (Figure 2A), indicating that this motif, as a specific aa sequence of the family, is closely related to its biological function and sequence characteristics. The aa composition analysis of the PSPG-box motifs showed that 44 aa made up the PSPG-box motif, some of which were highly conserved and related to the binding of sugar donors, including positions 1 (W), 4 (Q), 8 (L), 10 (H), 19 (H), 21–24 (GWNS), 27 (E), 32–34 (GVP), 39 (P), 43 (D/E), and 44 (Q) (Figure 2B) [57]. In addition, members in different evolutionary groups showed differences in the distribution of conserved motifs. For example, except for groups A, I, M, N, and R, most members of other groups contained motif 10; only members of groups A, C, I, M, and P did not have motif 17; motif 12 was only found in groups E, G, and P; and members of groups F and R did not have motif 9. The differences in the distribution of these motifs may be related to the different biological functions of the members of each group. Members of the same group had similar motif types and arrangement sequences, indicating a close evolutionary relationship between members of the same subgroup. An exon–intron analysis indicated that most members of the same group had similar intron numbers, with 52 out of 120 *PgUGT*s having no introns, including the members of groups B and R (Figure 2C).

3.3. Gene Duplication and Synteny Analysis of PgUGTs

Genome location analyses showed that 98 *PgUGT*s were distributed on nine pomegranate chromosomes, and the other *PgUGT*s were distributed on scaffolds (Figure 3A). Chromosome 3 contained the most *PgUGT*s (20), followed by chromosome 4 (13) and chromosomes 1 and 2 (12 each). Only one *PgUGT* was distributed on chromosome 8. For the same group of genes, the distribution of chromosomes was irregular. For example, members of groups E, L, and G were distributed on seven, five, and six chromosomes, respectively. There were also some *PgUGT*s distributed on chromosomes as gene clusters.

Gene duplication promotes the evolution of gene families. The duplication mode mainly includes tandem duplication, fragment duplication, genome-wide duplication, and rearrangement at the chromosome. Groups E, A, D, L, H, and P possessed the maximum number of tandem duplicated *UGT*s (five, three, three, three, two, and two, respectively), and B, C, G, N, and R possessed one only (Figure 3A). Groups F, I, J, and M did not have any tandem duplicated UGTs. A total of seven pairs of duplication genes were identified from the pomegranate *UGT* family, all of which were fragment duplication: *Pgr013573.1/Pgr004004.1*, *Pgr014646.1/Pgr008782.1*, *Pgr022566.1/Pgr025860.1*, *Pgr004136.1/Pgr003390.1*, *Pgr007463.1/Pgr002854.1*, *Pgr022563.1/Pgr007805.1*, and *Pgr010381.1/Pgr025860.1* (Figure 3B). These results suggest that tandem duplication and fragment duplication played important roles in the expansion of the *PgUGT* family. The Ka/Ks values of duplication gene pairs were calculated using TBtools (Table S3). Seven duplication gene pairs had Ka/Ks < 1, indicating that the *PgUGT* family was mainly affected by purifying selection during the evolution process.

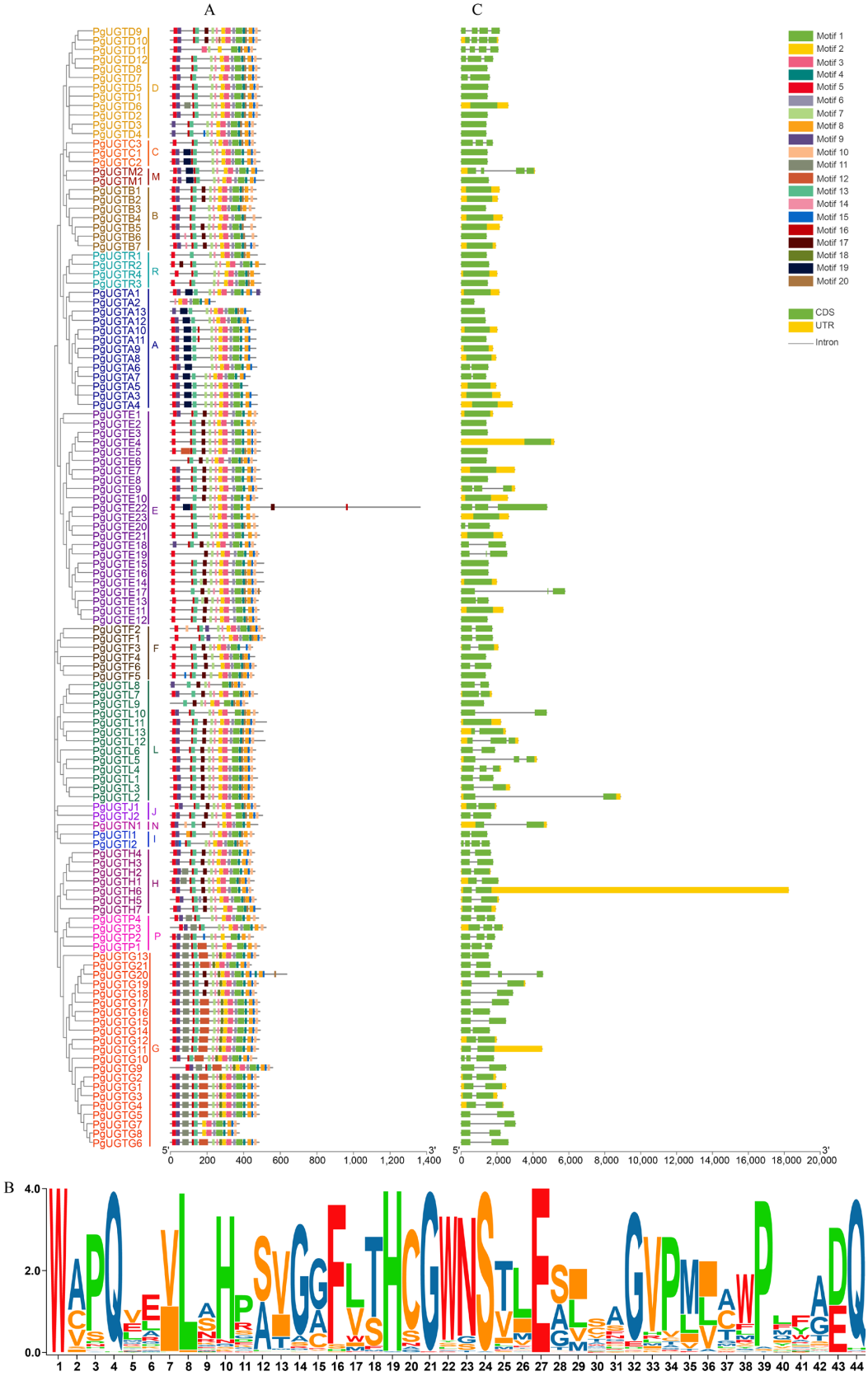

Figure 2. Conserved motifs and gene structure analysis of *PgUGT*s. (**A**) Distribution of the conserved motif for PgUGT proteins. The capital letters(A–J, L–N, P, and R) represent different groups. (**B**) Amino acid composition analysis of motif 1 (PSPG-box). (**C**) Gene structure of *PgUGT*s.

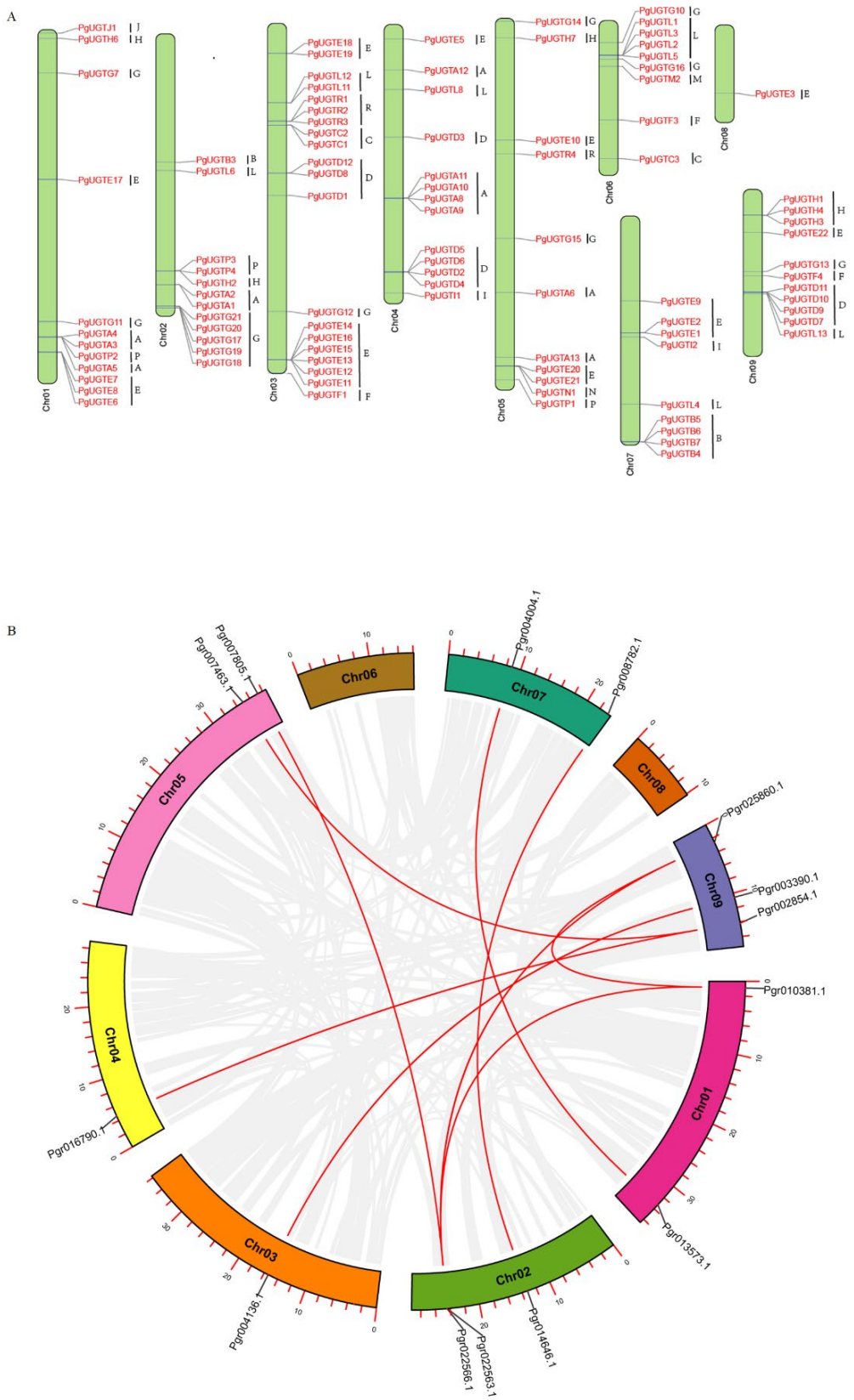

Figure 3. Chromosome distribution and collinearity analysis of *PgUGT*s. (**A**) The *PgUGT*s were mapped to different chromosomes. The capital letters (A–J, L–N, P, and R) represent different groups. (**B**) Collinearity analysis of *PgUGT*s in pomegranate. The red lines highlight the syntenic gene pairs.

3.4. Expression Profiles of *PgUGT*s Based on RNA-seq Data

To investigate the potential functions of the *PgUGT*s, we analyzed their transcript abundances using two sets of published RNA-seq data. First, we detected the expression profiles of 120 *PgUGT*s in different pomegranate tissues: root, leaf, flower, peel, and outer and inner seed coats (Figure 4A). A total of 46 *PgUGT*s were expressed in all six tissues, while 20 *PgUGT*s had no transcript abundance in all these tissues. Some *PgUGT*s showed tissue-specific expression, for example, *PgUGTG1*, *PgUGTG2*, *PgUGTG3*, *PgUGTL2*, and *PgUGTE18* were specifically expressed in roots; *PgUGTE7*, *PgUGTE16*, *PgUGTH2*, *PgUGTL4*, and *PgUGTL10* were mainly expressed in leaves; *PgUGTR4*, *PgUGTD7*, *PgUGTN1*, *PgUGTA13*, and *PgUGTF3* were specifically expressed in flowers; and *PgUGTG5*, *PgUGTG12*, and *PgUGTM2* were specifically expressed in peel. In addition, some *PgUGT*s showed expression in seed coats: *PgUGTE12*, *PgUGTG9*, and *PgUGTL13* had higher expression levels in the outer than the inner seed coat, while *PgUGTE20*, *PgUGTE21*, *PgUGTL6*, and *PgUGTL11* had higher expression levels in the inner than the outer seed coat.

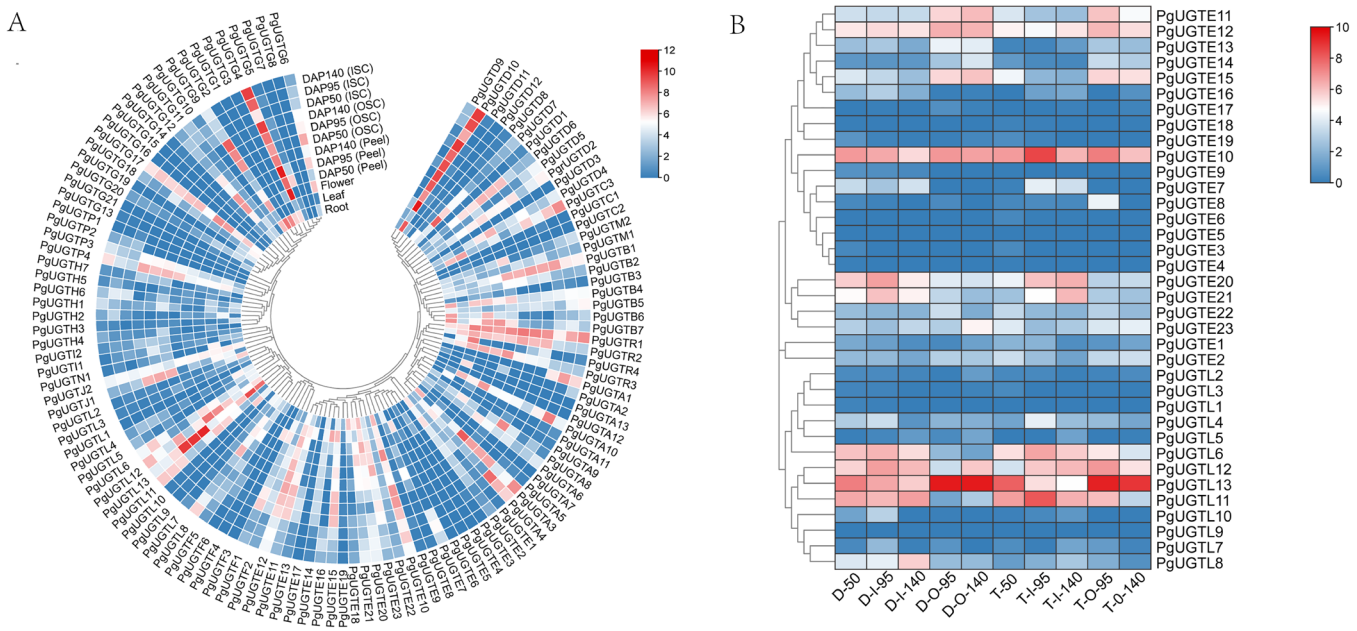

Figure 4. Expression profiles of *PgUGT*s. (**A**) Expression profiles of *PgUGT*s in different tissues. Transcript data of *PgUGT*s in root, flower, leaf, peel, and inner and outer seed coat at 50, 95, and 140 days after pollination (DAP) were normalized with $\log_2$ transformed FPKM values. ISC, inner seed coat; and OSC, outer seed coat. (**B**) Expression profiles of the *PgUGT*s of groups L and E in seed coats of soft-seeded 'Tunisia' and hard-seeded 'Dabenzi'. The transcript data of *PgUGT*s in the inner and outer seed coats of 'Dabenzi' and 'Tunisia' at 50, 95, and 140 DAP were normalized with $\log_2$ transformed FPKM values. D, 'Dabenzi'; T, 'Tunisia'; DAP, days after pollination; I, inner seed coat; and O, outer seed coat.

The *PgUGT*s distributed in groups E and L were considered responsible for the glycosylation modification of monolignols/precursors and hormones [27,28,35,58–60]. Therefore, we focused on the members of these two groups for investigating spatiotemporal expression patterns in the seed coats of the hard-seeded cultivar 'Dabenzi' and the soft-seeded cultivar 'Tunisia' at three developmental stages. Eight *PgUGT*s (*PgUGTE10*, *PgUGTE12*, *PgUGTE20*, *PgUGTE21*, *PgUGTL6*, *PgUGTL11*, *PgUGTL12*, and *PgUGTL13*) were highly expressed in seed coats of both cultivars (Figure 4B): *PgUGTE20*, *PgUGTE21*, *PgUGTL6*, *PgUGTL11*, and *PgUGTL12* were mainly expressed in the inner seed coat, while *PgUGTE12* and *PgUGTL13* were mainly expressed in the outer seed coat. The relative expression levels of *PgUGTE10* and *PgUGTL11* in the inner seed coat of 'Tunisia' were higher than

in 'Dabenzi'. Accordingly, these eight genes were selected for further study as candidate genes involved in seed hardness development.

3.5. CRE Identification and Relative Expression of PgUGTs Responding to Exogenous Hormones

The CREs in the promoter regions were identified to investigate the transcriptional regulation of the candidate *PgUGT*s (Figure 5). Several light-responsive elements were present in the *PgUGT*s. Nine elements related to hormones were identified, including TGA-box, TGA element, and AuxRR-core, which respond to auxin [61]; P-box, TATC-box, and GARE-motif, which respond to gibberellin [62]; TCA-element that responds to salicylic acid [63]; ABRE that responds to abscisic acid [64]; and CGTCA-motif that responds to methyl jasmonate [65]. There were five CREs related to plant growth and development: CAT-box, A-box, GCN4-motif, O2-site, and MBSI [66–68]. Interestingly, *PgUGTL11* contained MBSI elements, indicating that it may participate in the phenylpropanoid pathway.

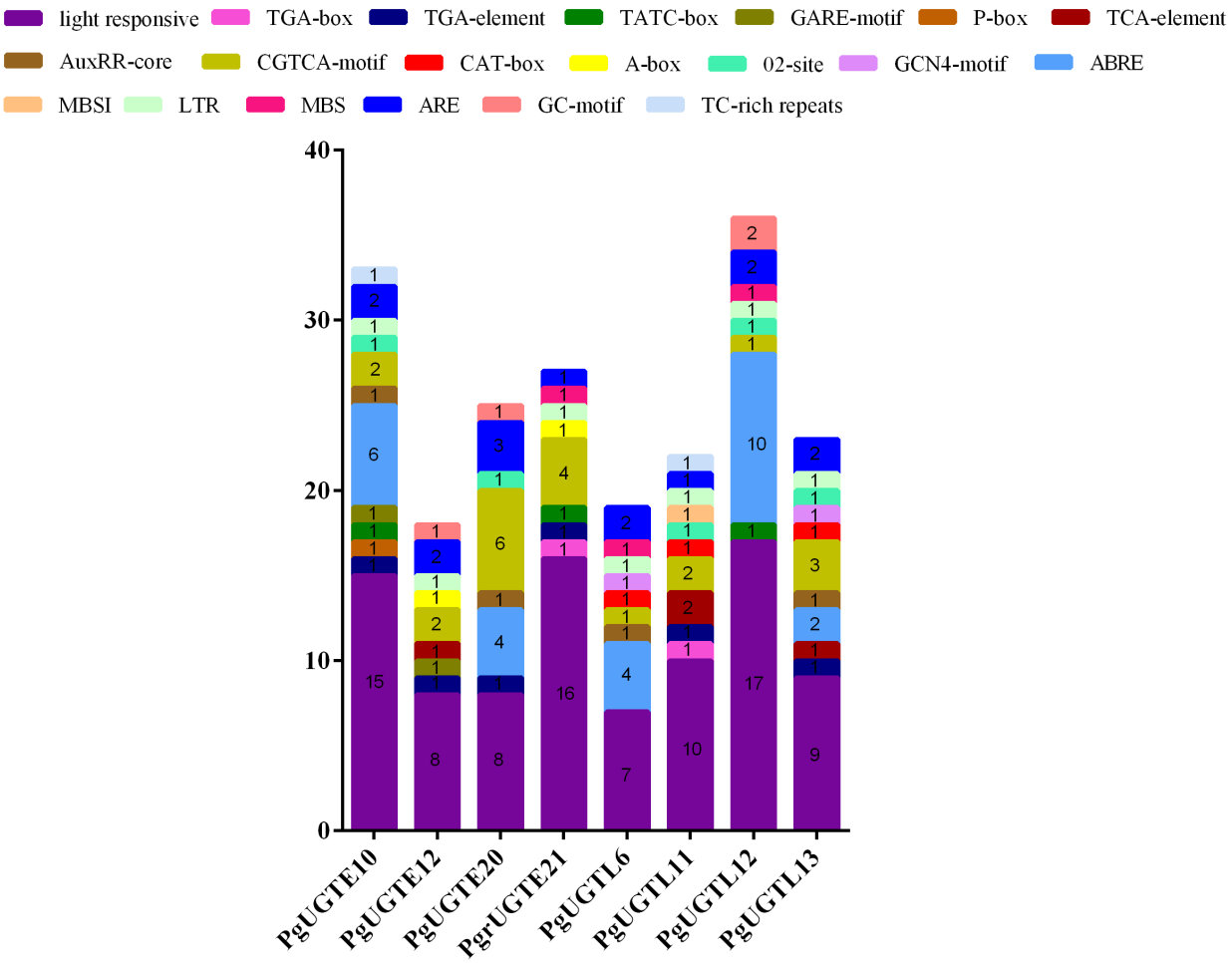

Figure 5. CREs of the candidate *PgUGT*s. The CREs are displayed in different colored boxes. The number of each CRE in the gene is displayed in the boxes.

We studied the expression levels of eight candidate *PgUGT*s under IAA and BR treatments. The expression levels of *PgUGTE20*, *PgUGTE21*, and *PgUGTL11* were induced by IAA (Figure 6A), while *PgUGTE10*, *PgUGTE20*, *PgUGTL11*, and *PgUGTL12* were up-regulated by BR (Figure 6B).

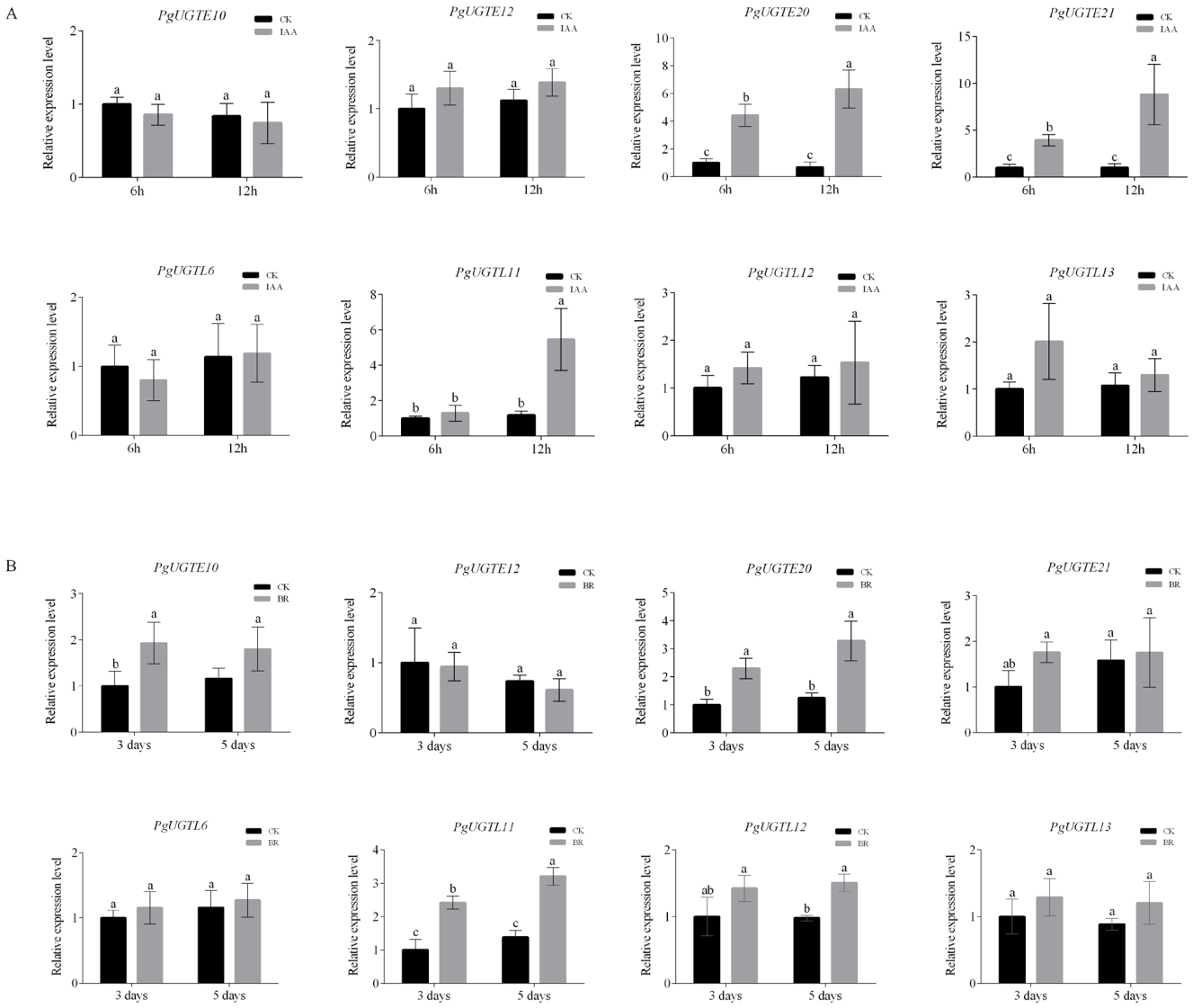

Figure 6. Expression analysis of *PgUGT*s under hormone treatment by qRT-PCR. (**A**) Relative expression levels of candidate *PgUGT*s in response to auxin treatment after 6 and 12 h. (**B**) Relative expression levels of candidate *PgUGT*s in response to BR treatment after 3 and 5 days. IAA, auxin; BR, brassinolide. Error bars indicate the standard deviation of three replications. Different letters indicate a significant difference at $p < 0.05$ using Tukey's test.

3.6. Co-Expression Analysis of Candidate PgUGTs

According to the expression profiles of *PgUGT*s, *PgUGTE10* and *PgUGTL11* were selected to perform co-expression analysis between candidate *PgUGT*s and genes enriched in phenylpropanoid biosynthesis and hormone signaling pathways. The gene *PgUGTL11* was co-expressed with 26 genes involved in the hormone-signaling and lignin biosynthesis pathways (Figure 7), including the *Pgr006318.1*- and *Pgr006319.1*-encoding cinnamyl-alcohol dehydrogenase, *Pgr016121.1*-encoding cinnamoyl-CoA reductase, *Pgr011171.1*-encoding peroxiredoxin, *Pgr000815.1*-encoding IAA-responsive protein, and *Pgr001703.1*-encoding the auxin-responsive protein. The gene *PgUGTE10* was co-expressed with six genes, including the *Pgr014360.1*-encoding shikimate O-hydroxycinnamoyl transferase, *Pgr013400.1*-encoding cinnamyl-alcohol dehydrogenase, and *Pgr011628.1*-encoding auxin-response factor (Figure 7). The functional annotation of these co-expression genes is shown in Table S4.

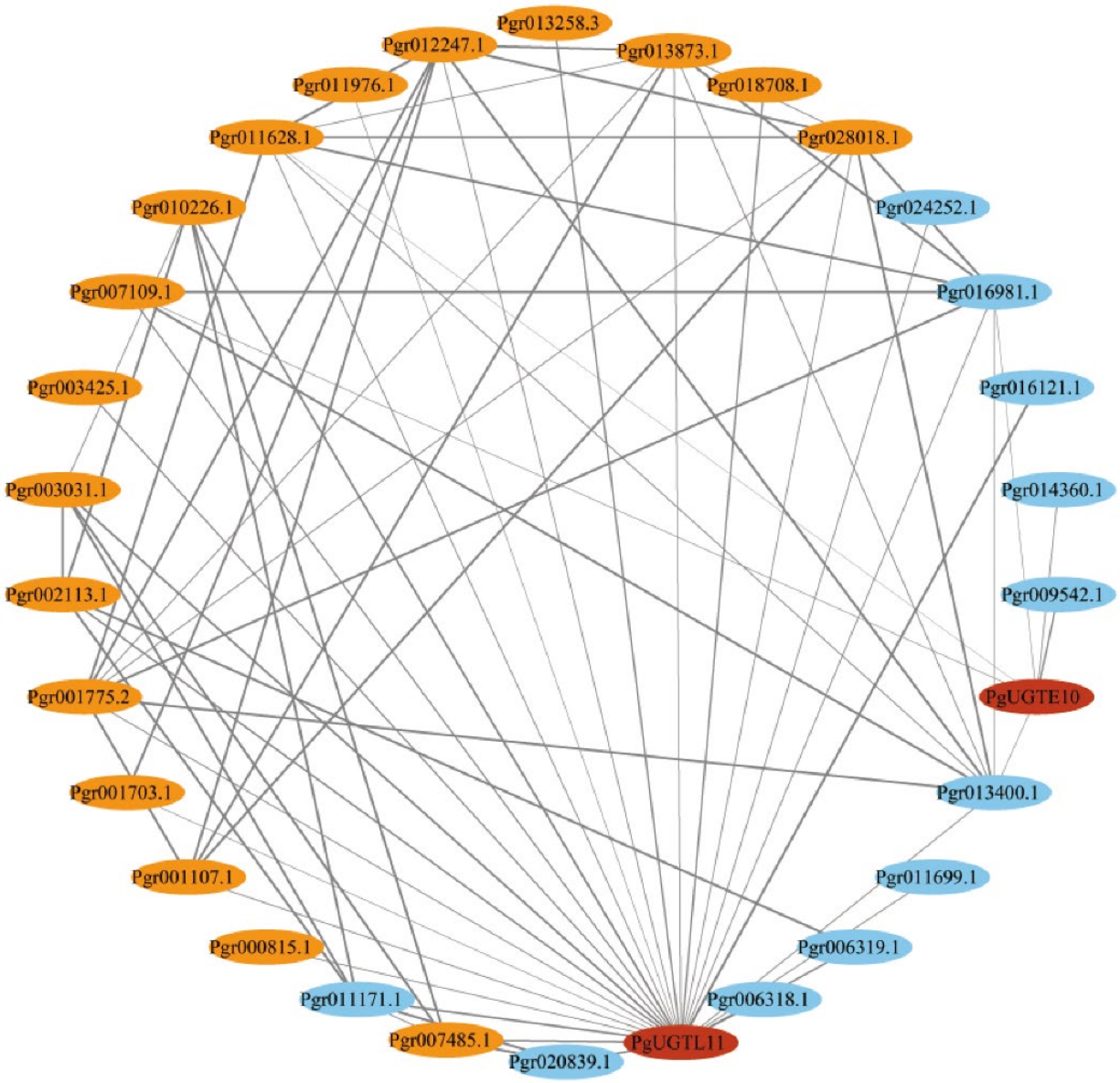

Figure 7. Co-expression network of candidate *PgUGT*s and genes involved in phenylpropanoid biosynthesis and hormone signaling pathways. The red nodes represent the *PgUGT*s, orange nodes represent genes involved in the hormone signaling pathway, and blue nodes represent genes involved in the phenylpropanoid biosynthesis pathway. The thickness of lines represents Pearson's correlation coefficients.

3.7. Subcellular Localization of PgUGTL11 and PgUGTE10

To investigate the subcellular localization of *PgUGTL11* and *PgUGTE10*, we constructed *35S::PgUGTL11/PgUGTE10–GFP* fusion vectors and transformed them into tobacco epidermal cells. The results showed that PgUGTL11–GFP and PgUGTE10–GFP presented green fluorescent signals in the nucleus, plasma membrane, and cytoplasm, similar to the control GFP signals (Figure 8).

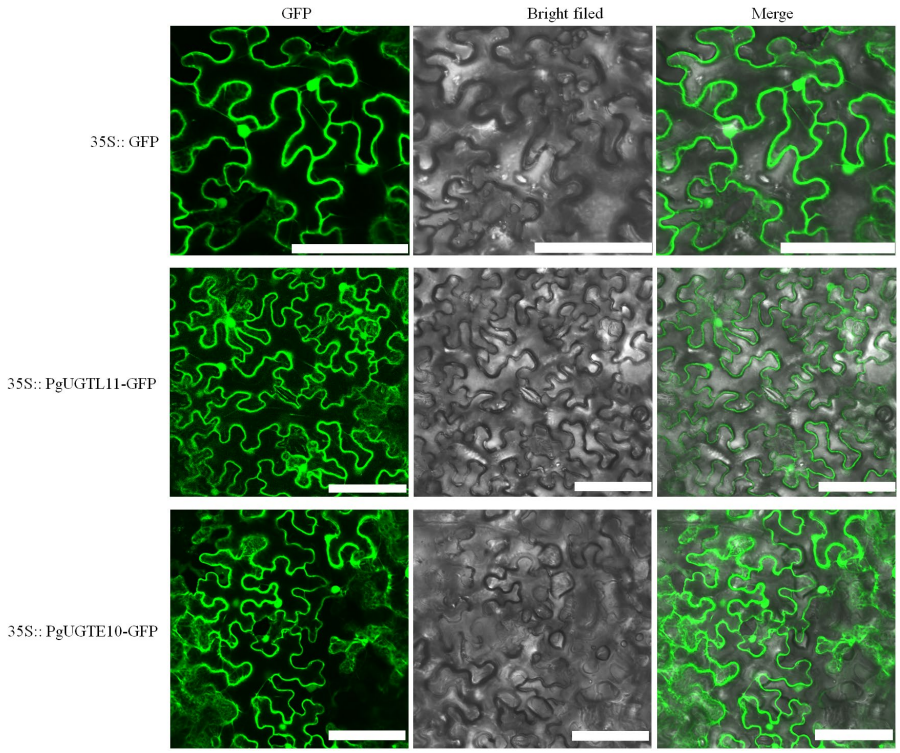

Figure 8. Subcellular localization of PgUGTL11 and PgUGTE10 in tobacco epidermal cells. Scale bar, 100 μm.

4. Discussion

Glycosylation modification is ubiquitous in secondary plant metabolites and determines the complex and diverse regulatory network of natural plant products [69]. Glycosylation is involved in regulating the bioactivity of hormones, in the detoxification of xenobiotics, as well as in the biosynthesis, storage, and transport properties of secondary metabolites, suggesting an important role in plant growth and development [70–72]. The *UGT* family is a multigene family of glycosyltransferases with a broad range of substrates [21,22]. In recent years, the *UGT* family has been identified in plant species, including *Arabidopsis* [46], rice [26], soybean [73], and fruit species such as grape [21], apple [56], and pear [74]. In pomegranate, three *UGT*s were identified, but the large-scale analysis was missing.

We identified 120 *PgUGT*s in the pomegranate genome. Phylogenetic analysis showed the *PgUGT*s were divided into 15 groups, including 13 conserved groups (A–J and L–N) and two newly discovered groups (P and R). The P group is also found in some other species, including rice [26], grape [75], and apple [56]. The R group is not found in many species but is present in tea [24]. In contrast, groups K and O are present in many species but not in pomegranates. In addition, group G contained 21 *PgUGT*s but only six *AtUGT*s, and group H contained only seven *PgUGT*s but 19 *AtUGT*s. These findings suggest that specific expansion or gene loss events of the *UGT* family may have occurred in the evolution of different species. The main driving force of genome and genetic system evolution is gene replication, which promotes plant evolution and leads to the expansion of gene families [76]. The 59 *PgUGT*s involved in 23 tandem duplication events and the seven pairs of segment duplication genes suggest that tandem duplication and fragment duplication may have been the primary driving force for the expansion of the *PgUGT*s. The Ka/Ks ≤ 1 of *PgUGT* repeat gene pairs indicated that the *PgUGT* family eliminates harmful mutations through purification selection during evolution. The conserved motifs and gene structure analysis showed that all PgUGT protein sequences contained motif 1, a conserved sequence reported as essential for the binding of glycosyl groups. The PgUGT proteins in different phylogenetic groups contained different types and amounts of motifs. In addition, 52 (43%)

*PgUGT*s distributed in different phylogenetic groups did not contain any introns. The diversity of protein and gene structure suggests functional variation in the evolution of this gene family.

The structure and molecular composition of the seed coat profoundly affect seed physiology and have evolved to adapt to diverse environments [77]. The natural diversity of the seed coat structure affects the resistance, dormancy, and germination of seeds [78–80]. Angiosperms have evolved two integuments (bitegmic), which develop into the so-called inner and outer seed coats [77]. Interestingly, unlike most angiosperms, the outer seed coat of pomegranate is soft and juicy, and the inner seed coat is highly lignified. The distinguishing structure characteristics of inner and outer seed coats are due to the differential cell expansion and differential accumulation of cellular metabolites, especially of monolignols/monolignol glucosides [53]. However, the molecular regulation mechanism of seed coat development in pomegranate remains unclear. In this study, we attempted to identify candidate *PgUGT*s involved in seed coat development, especially seed hardness development. We focused on the *PgUGT*s in phylogenetic groups E and L, which were reported for the glycosylation modification of monolignols/precursors and hormones. We found that eight *PgUGT*s in these two groups were expressed in seed coats. Among them, *PgUGTL11* and *PgUGTE10* showed higher expression levels in the seed coat of soft-seeded 'Tunisia' compared to the hard-seeded 'Dabenzi'. The *AtUGT*s with high homology to *PgUGTL11* (i.e., *AtUGT84B1* and *AtUGT84B2*) were reported to glycosylate IAA in vitro and play crucial roles in regulating IAA homeostasis in plants [33,34,81]. The homologous gene cluster *AtUGT84A1–4* of *PgUGTL11* can glycosylate monolignol precursors [27]. Gene *AtUGT72B1*, homologous to *PgUGTE10*, regulates cell wall lignification by glycosylating coniferyl alcohol [30]. In addition, a cluster of homologous *AtUGT*s, including *AtUGT72E1*, *AtUGT72E2*, and *AtUGT72E3*, was identified as responsible for glucose conjugation of monolignols [29,82]. We found that expression levels of *PgUGTE10* were induced by BR treatment, while *PgUGTL11* expression was up-regulated both by IAA and BR treatment. In addition, *PgUGTL11* and *PgUGTE10* were co-expressed with the genes involved in phenylpropanoid biosynthesis and hormone signaling pathways. Auxin has been proven to play a crucial role in seed coat initiation and development by regulating various physiological processes, including cell expansion and lignin biosynthesis [9,83,84]. Several genes involved in lignin synthesis were regulated by BR, thereby promoting cellular lignification and xylem vessel formation [85–87]. The UGT proteins are localized in the nucleus, cytoplasm, chloroplast, and other regions, and tend to have substrate diversity, which may be beneficial for metabolic regulation in plants [88–90]. Both PgUGTL11 and PgUGTE10 may be localized in the nucleus, plasma membrane, and cytoplasm, but the exact localization requires further verification. Thus, *PgUGTL11* and *PgUGTE10* are potential candidate genes involved in seed hardness development through glycosylating specific substrates, possibly hormones or monolignols.

5. Conclusions

We identified 120 *UGT* genes in pomegranate, which were divided into 15 groups according to phylogenetic analysis. Tandem duplication and fragment duplication played important roles in the expansion of the *PgUGT* gene family. The *PgUGT*s exhibited various expression profiles in different pomegranate tissues. Comprehensive analysis indicated that *PgUGTL11* and *PgUGTE10* are potential candidate genes involved in seed hardness development. These results provide new insights into the characteristics of the *PgUGT* family and its potential functions in pomegranate seed coat development.

Supplementary Materials: The following supporting information can be downloaded at: https://www.mdpi.com/article/10.3390/horticulturae9010119/s1, Figure S1. The phylogenetic tree of UGTs in newly discovered groups P and R in pomegranate, apple, and tea. Table S1. The gene-specific primers used in this study. Table S2. Detailed information of PgUGTs identified in the pomegranate genome. Table S3. Ka/Ks analysis of PgUGT duplicated genes. Table S4. The functional annotation of the genes that co-expressed with the candidate PgUGTs.

Author Contributions: Conceptualization, J.L. and G.Q.; data curation, G.L. and J.L.; methodology, G.L., J.L. and X.L.; resources, Z.C. and B.J.; supervision, C.L.; writing—original draft, G.L. and J.L.; writing—review and editing, G.Q. and H.Z. All authors have read and agreed to the published version of the manuscript.

Funding: This research was supported by the Major Science and Technology Project of Anhui Province (201903b06020017), the Major Science and Technology Project of Huaibei City (HK2021014), and the Natural Science Foundation of Anhui Province (2108085QC129).

Institutional Review Board Statement: Not applicable.

Informed Consent Statement: Not applicable.

Data Availability Statement: All datasets presented in this study are included in the article/ Supplementary Material.

Conflicts of Interest: The authors declare no conflict of interest.

References

1. Niu, J.; Cao, D.; Li, H.; Xue, H.; Chen, L.; Liu, B.; Cao, S. Quantitative proteomics of pomegranate varieties with contrasting seed hardness during seed development stages. *Tree Genet. Genomes* **2018**, *14*, 14. [CrossRef]
2. Heber, D. Multitargeted therapy of cancer by ellagitannins. *Cancer Lett.* **2008**, *269*, 262–268. [CrossRef] [PubMed]
3. Xie, X.; Huang, Y.; Tian, S.; Li, G.; Cao, S. Relationship of seed hardness development and microstructure of seed coat cell in soft seed pomegranate. *Acta Hortic. Sin.* **2017**, *44*, 1174–1180. [CrossRef]
4. Boerjan, W.; Ralph, J.; Baucher, M. Lignin biosynthesis. *Annu. Rev. Plant Biol.* **2003**, *54*, 519–546. [CrossRef] [PubMed]
5. Liu, C.J.; Miao, Y.C.; Zhang, K.W. Sequestration and transport of lignin monomeric precursors. *Molecules* **2011**, *16*, 710–727. [CrossRef]
6. Dima, O.; Morreel, K.; Vanholme, B.; Kim, H.; Ralph, J.; Boerjan, W. Small glycosylated lignin oligomers are stored in *Arabidopsis* leaf vacuoles. *Plant Cell* **2015**, *27*, 695–710. [CrossRef]
7. Luo, M.; Dennis, E.S.; Berger, F.; Peacock, W.J.; Chaudhury, A. MINISEED3 (MINI3), a WRKY family gene, and HAIKU2 (IKU2), a leucine-rich repeat (LRR) KINASE gene, are regulators of seed size in *Arabidopsis*. *Proc. Natl. Acad. Sci. USA* **2005**, *102*, 17531–17536. [CrossRef]
8. Garcia, D.; Saingery, V.; Chambrier, P.; Mayer, U.; Jurgens, G.; Berger, F. Arabidopsis haiku mutants reveal new controls of seed size by endosperm. *Plant Physiol.* **2003**, *131*, 1661–1670. [CrossRef]
9. Figueiredo, D.D.; Batista, R.A.; Roszakt, P.J.; Hennig, L.; Kohler, C. Auxin production in the endosperm drives seed coat development in *Arabidopsis*. *Elife* **2016**, *5*, e20542. [CrossRef]
10. Immanen, J.; Nieminen, K.; Smolander, O.P.; Kojima, M.; Serra, J.A.; Koskinen, P.; Zhang, J.; Elo, A.; Mahonen, A.P.; Street, N.; et al. Cytokinin and auxin display distinct but interconnected distribution and signaling profiles to stimulate cambial activity. *Curr. Biol.* **2016**, *26*, 1990–1997. [CrossRef]
11. Xu, C.Z.; Shen, Y.; He, F.; Fu, X.K.; Yu, H.; Lu, W.X.; Li, Y.L.; Li, C.F.; Fan, D.; Wang, H.C.; et al. Auxin-mediated Aux/IAA-ARF-HB signaling cascade regulates secondary xylem development in Populus. *New Phytol.* **2019**, *222*, 752–767. [CrossRef]
12. Uggla, C.; Mellerowicz, E.J.; Sundberg, B. Indole-3-acetic acid controls cambial growth in Scots pine by positional signaling. *Plant Physiol.* **1998**, *117*, 113–121. [CrossRef]
13. Korasick, D.A.; Enders, T.A.; Strader, L.C. Auxin biosynthesis and storage forms. *J. Exp. Bot.* **2013**, *64*, 2541–2555. [CrossRef]
14. Jin, H.; Do, J.; Shin, S.J.; Choi, J.W.; Choi, Y.I.; Kim, W.; Kwon, M. Exogenously applied 24-epi brassinolide reduces lignification and alters cell wall carbohydrate biosynthesis in the secondary xylem of Liriodendron tulipifera. *Phytochemistry* **2014**, *101*, 40–51. [CrossRef]
15. Ge, Y.H.; Li, C.Y.; Tang, R.X.; Sun, R.H.; Li, J.R. Effects of postharvest brassinolide dipping on quality parameters and antioxidant activity in peach fruit. In Proceedings of the 3rd International Symposium on Postharvest Pathology—Using Science to Increase Food Availability, Bari, Italy, 7–11 June 2015; pp. 377–384. [CrossRef]
16. Sanchez-Rodriguez, C.; Rubio-Somoza, I.; Sibout, R.; Persson, S. Phytohormones and the cell wall in *Arabidopsis* during seedling growth. *Trends Plant Sci.* **2010**, *15*, 291–301. [CrossRef]
17. Ibanes, M.; Fabregas, N.; Chory, J.; Cano-Delgado, A.I. Brassinosteroid signaling and auxin transport are required to establish the periodic pattern of Arabidopsis shoot vascular bundles. *Proc. Natl. Acad. Sci. USA* **2009**, *106*, 13630–13635. [CrossRef]
18. Oda, Y.; Mimura, T.; Hasezawa, S. Regulation of secondary cell wall development by cortical microtubules during tracheary element differentiation in *Arabidopsis* cell suspensions. *Plant Physiol.* **2005**, *137*, 1027–1036. [CrossRef]
19. Shen, H.; Mazarei, M.; Hisano, H.; Escamilla-Trevino, L.; Fu, C.X.; Pu, Y.Q.; Rudis, M.R.; Tang, Y.H.; Xiao, X.R.; Jackson, L.; et al. A genomics approach to deciphering lignin biosynthesis in switchgrass. *Plant Cell* **2013**, *25*, 4342–4361. [CrossRef]
20. Ostrowski, M.; Jakubowska, A. UDP-Glycosyltransferases of Plant Hormones. *Postep. Biol. Komorki* **2013**, *40*, 141–160. [CrossRef]
21. Yonekura-Sakakibara, K.; Hanada, K. An evolutionary view of functional diversity in family 1 glycosyltransferases. *Plant J.* **2011**, *66*, 182–193. [CrossRef]

22. Paquette, S.; Møller, B.L.; Bak, S. On the origin of family 1 plant glycosyltransferases. *Phytochemistry* **2003**, *62*, 399–413. [CrossRef] [PubMed]
23. Ross, J.; Li, Y.; Lim, E.-K.; Bowles, D.J. Higher plant glycosyltransferases. *Genome Biol.* **2001**, *2*, reviews3004.1. [CrossRef] [PubMed]
24. Cui, L.; Yao, S.; Dai, X.; Yin, Q.; Liu, Y.; Jiang, X.; Wu, Y.; Qian, Y.; Pang, Y.; Gao, L.; et al. Identification of UDP-glycosyltransferases involved in the biosynthesis of astringent taste compounds in tea (*Camellia sinensis*). *J. Exp. Bot.* **2016**, *67*, 2285–2297. [CrossRef] [PubMed]
25. Li, Y.; Li, P.; Wang, Y.; Dong, R.; Yu, H.; Hou, B. Genome-wide identification and phylogenetic analysis of family-1 UDP glycosyltransferases in maize (*Zea mays*). *Planta* **2014**, *239*, 1265–1279. [CrossRef]
26. Caputi, L.; Malnoy, M.; Goremykin, V.; Nikiforova, S.; Martens, S. A genome-wide phylogenetic reconstruction of family 1 UDP-glycosyltransferases revealed the expansion of the family during the adaptation of plants to life on land. *Plant J.* **2012**, *69*, 1030–1042. [CrossRef]
27. Lim, E.-K.; Li, Y.; Parr, A.; Jackson, R.; Ashford, D.A.; Bowles, D.J. Identification of glucosyltransferase genes involved in sinapate metabolism and lignin synthesis in *Arabidopsis*. *J. Biol. Chem.* **2001**, *276*, 4344–4349. [CrossRef]
28. Lim, E.-K.; Jackson, R.G.; Bowles, D.J. Identification and characterisation of Arabidopsis glycosyltransferases capable of glucosylating coniferyl aldehyde and sinapyl aldehyde. *FEBS Lett.* **2005**, *579*, 2802–2806. [CrossRef]
29. Lanot, A.; Hodge, D.; Jackson, R.G.; George, G.L.; Elias, L.; Lim, E.K.; Vaistij, F.E.; Bowles, D.J. The glucosyltransferase UGT72E2 is responsible for monolignol 4-O-glucoside production in *Arabidopsis thaliana*. *Plant J.* **2006**, *48*, 286–295. [CrossRef]
30. Lin, J.S.; Huang, X.X.; Li, Q.; Cao, Y.; Bao, Y.; Meng, X.F.; Li, Y.J.; Fu, C.; Hou, B.K. UDP-glycosyltransferase 72B1 catalyzes the glucose conjugation of monolignols and is essential for the normal cell wall lignification in *Arabidopsis thaliana*. *Plant J.* **2016**, *88*, 26–42. [CrossRef]
31. Wang, H.; Feng, X.; Zhang, Y.; Wei, D.; Zhang, Y.; Jin, Q.; Cai, Y. PbUGT72AJ2-mediated glycosylation plays an important role in lignin formation and stone cell development in pears (*Pyrus bretschneideri*). *Int. J. Mol. Sci.* **2022**, *23*, 7893. [CrossRef]
32. Szerszen, J.B.; Szczyglowski, K.; Bandurski, R.S. iaglu, a gene from Zea mays involved in conjugation of growth hormone indole-3-acetic acid. *Science* **1994**, *265*, 1699–1701. [CrossRef]
33. Jackson, R.G.; Lim, E.-K.; Li, Y.; Kowalczyk, M.; Sandberg, G.; Hoggett, J.; Ashford, D.A.; Bowles, D.J. Identification and biochemical characterization of an Arabidopsis indole-3-acetic acid glucosyltransferase. *J. Biol. Chem.* **2001**, *276*, 4350–4356. [CrossRef]
34. Jackson, R.G.; Kowalczyk, M.; Li, Y.; Higgins, G.; Ross, J.; Sandberg, G.; Bowles, D.J. Over-expression of an Arabidopsis gene encoding a glucosyltransferase of indole-3-acetic acid: Phenotypic characterisation of transgenic lines. *Plant J.* **2002**, *32*, 573–583. [CrossRef]
35. Tognetti, V.B.; Van Aken, O.; Morreel, K.; Vandenbroucke, K.; van de Cotte, B.; De Clercq, I.; Chiwocha, S.; Fenske, R.; Prinsen, E.; Boerjan, W.; et al. Perturbation of indole-3-butyric acid homeostasis by the UDP-glucosyltransferase UGT74E2 modulates Arabidopsis architecture and water stress tolerance. *Plant Cell* **2010**, *22*, 2660–2679. [CrossRef]
36. Jin, S.-H.; Ma, X.-M.; Han, P.; Wang, B.; Sun, Y.-G.; Zhang, G.-Z.; Li, Y.-J.; Hou, B.-K. UGT74D1 is a novel auxin glycosyltransferase from Arabidopsis thaliana. *PLoS ONE* **2013**, *8*, e61705. [CrossRef]
37. Poppenberger, B.; Fujioka, S.; Soeno, K.; George, G.L.; Vaistij, F.E.; Hiranuma, S.; Seto, H.; Takatsuto, S.; Adam, G.; Yoshida, S. The UGT73C5 of Arabidopsis thaliana glucosylates brassinosteroids. *Proc. Natl. Acad. Sci. USA* **2005**, *102*, 15253–15258. [CrossRef]
38. Husar, S.; Berthiller, F.; Fujioka, S.; Rozhon, W.; Khan, M.; Kalaivanan, F.; Elias, L.; Higgins, G.S.; Li, Y.; Schuhmacher, R. Overexpression of the UGT73C6 alters brassinosteroid glucoside formation in *Arabidopsis thaliana*. *BMC Plant Biol.* **2011**, *11*, 51. [CrossRef]
39. Ono, N.N.; Qin, X.; Wilson, A.E.; Li, G.; Tian, L. Two UGT84 family glycosyltransferases catalyze a critical reaction of hydrolyzable tannin biosynthesis in pomegranate (*Punica granatum*). *PLoS ONE* **2016**, *11*, e0156319. [CrossRef]
40. Wilson, A.E.; Wu, S.; Tian, L. PgUGT95B2 preferentially metabolizes flavones/flavonols and has evolved independently from flavone/flavonol UGTs identified in *Arabidopsis thaliana*. *Phytochemistry* **2019**, *157*, 184–193. [CrossRef]
41. Shi, M.; Liu, X.; Zhang, H.; He, Z.; Yang, H.; Chen, J.; Feng, J.; Yang, W.; Jiang, Y.; Yao, J.-L. The IAA-and ABA-responsive transcription factor CgMYB58 upregulates lignin biosynthesis and triggers juice sac granulation in pummelo. *Hortic. Res.* **2020**, *7*, 139. [CrossRef]
42. Soeno, K.; Fujioka, S.; Hiranuma, S.; Seto, H.; Yoshida, S. Metabolic conversion of castasterone and brassinolide into their glucosides in higher plants. *J. Plant Growth Regul.* **2006**, *25*, 195–202. [CrossRef]
43. Qin, G.; Xu, C.; Ming, R.; Tang, H.; Guyot, R.; Kramer, E.M.; Hu, Y.; Yi, X.; Qi, Y.; Xu, X. The pomegranate (*Punica granatum* L.) genome and the genomics of punicalagin biosynthesis. *Plant J.* **2017**, *91*, 1108–1128. [CrossRef] [PubMed]
44. Letunic, I.; Doerks, T.; Bork, P. SMART 7: Recent updates to the protein domain annotation resource. *Nucleic Acids Res.* **2012**, *40*, D302–D305. [CrossRef] [PubMed]
45. Marchler-Bauer, A.; Lu, S.; Anderson, J.B.; Chitsaz, F.; Derbyshire, M.K.; DeWeese-Scott, C.; Fong, J.H.; Geer, L.Y.; Geer, R.C.; Gonzales, N.R. CDD: A Conserved Domain Database for the functional annotation of proteins. *Nucleic Acids Res.* **2010**, *39*, D225–D229. [CrossRef] [PubMed]
46. Li, Y.; Baldauf, S.; Lim, E.K.; Bowles, D.J. Phylogenetic analysis of the UDP-glycosyltransferase multigene family of Arabidopsis thaliana. *J. Biol. Chem.* **2001**, *276*, 4338–4343. [CrossRef]

47. Bailey, T.L.; Boden, M.; Buske, F.A.; Frith, M.; Grant, C.E.; Clementi, L.; Ren, J.; Li, W.W.; Noble, W.S. MEME SUITE: Tools for motif discovery and searching. *Nucleic Acids Res.* **2009**, *37*, W202–W208. [CrossRef]
48. Chen, C.; Chen, H.; Zhang, Y.; Thomas, H.R.; Frank, M.H.; He, Y.; Xia, R. TBtools: An integrative toolkit developed for interactive analyses of big biological data. *Mol. Plant* **2020**, *13*, 1194–1202. [CrossRef]
49. Hoang, M.; Wu, C.-N.; Lin, C.-F.; Nguyen, H.T.T.; Chiou, M.-T.; Lin, C.-N. Genetic characterization of feline panleukopenia virus from dogs in Vietnam reveals a unique Thr101 mutation in VP2. *PeerJ* **2020**, *8*, e9752. [CrossRef]
50. Zhang, J. Evolution by gene duplication: An update. *Trends Ecol. Evol.* **2003**, *18*, 292–298. [CrossRef]
51. Zhang, Z.; Li, J.; Zhao, X.-Q.; Wang, J.; Wong, G.K.-S.; Yu, J. KaKs_Calculator: Calculating Ka and Ks through model selection and model averaging. *Genom. Proteom. Bioinform.* **2006**, *4*, 259–263. [CrossRef]
52. Lescot, M.; Déhais, P.; Thijs, G.; Marchal, K.; Moreau, Y.; Van de Peer, Y.; Rouzé, P.; Rombauts, S. PlantCARE, a database of plant cis-acting regulatory elements and a portal to tools for in silico analysis of promoter sequences. *Nucleic Acids Res.* **2002**, *30*, 325–327. [CrossRef]
53. Qin, G.; Liu, C.; Li, J.; Qi, Y.; Gao, Z.; Zhang, X.; Yi, X.; Pan, H.; Ming, R.; Xu, Y. Diversity of metabolite accumulation patterns in inner and outer seed coats of pomegranate: Exploring their relationship with genetic mechanisms of seed coat development. *Hortic. Res.* **2020**, *7*, 10. [CrossRef]
54. Kwiatkowska, M.; Norman, G.; Parker, D. PRISM 4.0: Verification of probabilistic real-time systems. In *Computer Aided Verification. CAV 2011. Lecture Notes in Computer Science*; Gopalakrishnan, G., Qadeer, S., Eds.; Springer: Berlin/Heidelberg, Germany, 2011; pp. 585–591.
55. Smoot, M.E.; Ono, K.; Ruscheinski, J.; Wang, P.L.; Ideker, T. Cytoscape 2.8: New features for data integration and network visualization. *Bioinformatics* **2011**, *27*, 431–432. [CrossRef]
56. Zhou, K.; Hu, L.; Li, P.; Gong, X.; Ma, F. Genome-wide identification of glycosyltransferases converting phloretin to phloridzin in *Malus species*. *Plant Sci.* **2017**, *265*, 131–145. [CrossRef]
57. Gachon, C.M.; Langlois-Meurinne, M.; Saindrenan, P. Plant secondary metabolism glycosyltransferases: The emerging functional analysis. *Trends Plant Sci.* **2005**, *10*, 542–549. [CrossRef]
58. Lim, E.-K.; Doucet, C.J.; Li, Y.; Elias, L.; Worrall, D.; Spencer, S.P.; Ross, J.; Bowles, D.J. The activity of Arabidopsis glycosyltransferases toward salicylic acid, 4-hydroxybenzoic acid, and other benzoates. *J. Biol. Chem.* **2002**, *277*, 586–592. [CrossRef]
59. Tanaka, K.; Hayashi, K.; Natsume, M.; Kamiya, Y.; Sakakibara, H.; Kawaide, H.; Kasahara, H. UGT74D1 catalyzes the glucosylation of 2-Oxindole-3-Acetic Acid in the auxin metabolic pathway in *Arabidopsis*. *Plant Cell Physiol.* **2014**, *55*, 218–228. [CrossRef]
60. Aoi, Y.; Hira, H.; Hayakawa, Y.; Liu, H.Q.; Fukui, K.; Dai, X.H.; Tanaka, K.; Hayashi, K.I.; Zhao, Y.D.; Kasahara, H. UDP-glucosyltransferase UGT84B1 regulates the levels of indole-3-acetic acid and phenylacetic acid in *Arabidopsis*. *Biochem. Biophys. Res. Commun.* **2020**, *532*, 244–250. [CrossRef]
61. Du, Y.; Zhao, Q.; Li, W.; Geng, J.; Li, S.; Yuan, X.; Gu, Y.; Zhong, J.; Zhang, Y.; Du, J. Genome-wide identification of the LBD transcription factor genes in common bean (*Phaseolus vulgaris* L.) and expression analysis under different abiotic stresses. *J. Plant Interact.* **2022**, *17*, 731–743. [CrossRef]
62. Pinweha, N.; Asvarak, T.; Viboonjun, U.; Narangajavana, J. Involvement of miR160/miR393 and their targets in cassava responses to anthracnose disease. *J. Plant Physiol.* **2015**, *174*, 26–35. [CrossRef]
63. Zeng, M.-H.; Liu, S.-H.; Yang, M.-X.; Zhang, Y.-J.; Liang, J.-Y.; Wan, X.-R.; Liang, H. Characterization of a gene encoding clathrin heavy chain in maize up-regulated by salicylic acid, abscisic acid and high boron supply. *Int. J. Mol. Sci.* **2013**, *14*, 15179–15198. [CrossRef] [PubMed]
64. Tuteja, N. Abscisic acid and abiotic stress signaling. *Plant Signal. Behav.* **2007**, *2*, 135–138. [CrossRef] [PubMed]
65. Xu, Z.; Sun, M.; Jiang, X.; Sun, H.; Dang, X.; Cong, H.; Qiao, F. Glycinebetaine biosynthesis in response to osmotic stress depends on jasmonate signaling in watermelon suspension cells. *Front. Plant Sci.* **2018**, *9*, 1469. [CrossRef] [PubMed]
66. Kaur, G.; Pati, P.K. Analysis of cis-acting regulatory elements of Respiratory burst oxidase homolog (Rboh) gene families in *Arabidopsis* and rice provides clues for their diverse functions. *Comput. Biol. Chem.* **2016**, *62*, 104–118. [CrossRef] [PubMed]
67. Kaur, A.; Pati, P.K.; Pati, A.M.; Nagpal, A.K. In-silico analysis of cis-acting regulatory elements of pathogenesis-related proteins of Arabidopsis thaliana and Oryza sativa. *PLoS ONE* **2017**, *12*, e0184523. [CrossRef]
68. Zhou, J.; Hu, Y.; Li, J.; Yu, Z.; Guo, Q. Genome-wide identification and expression analysis of the plant U-box protein gene family in *Phyllostachys edulis*. *Front. Genet.* **2021**, 2464. [CrossRef]
69. Song, C.K.; Gu, L.; Liu, J.Y.; Zhao, S.; Hong, X.T.; Schulenburg, K.; Schwab, W. Functional characterization and substrate promiscuity of UGT71 glycosyltransferases from strawberry (*Fragaria x ananassa*). *Plant Cell Physiol.* **2015**, *56*, 2478–2493. [CrossRef]
70. Lim, E.K.; Bowles, D.J. A class of plant glycosyltransferases involved in cellular homeostasis. *EMBO J.* **2004**, *23*, 2915–2922. [CrossRef]
71. Bowles, D.; Isayenkova, J.; Lim, E.K.; Poppenberger, B. Glycosyltransferases: Managers of small molecules. *Curr. Opin. Plant Biol.* **2005**, *8*, 254–263. [CrossRef]
72. Bowles, D.; Lim, E.K.; Poppenberger, B.; Vaistij, F.E. Glycosyltransferases of lipophilic small molecules. *Annu. Rev. Plant Biol.* **2006**, *57*, 567–597. [CrossRef]

73. Rehman, H.M.; Nawaz, M.A.; Bao, L.; Shah, Z.H.; Lee, J.-M.; Ahmad, M.Q.; Chung, G.; Yang, S.H. Genome-wide analysis of family-1 UDP-glycosyltransferases in soybean confirms their abundance and varied expression during seed development. *J. Plant Physiol.* **2016**, *206*, 87–97. [CrossRef]
74. Cheng, X.; Muhammad, A.; Li, G.; Zhang, J.; Cheng, J.; Qiu, J.; Jiang, T.; Jin, Q.; Cai, Y.; Lin, Y. Family-1 UDP glycosyltransferases in pear (*Pyrus bretschneideri*): Molecular identification, phylogenomic characterization and expression profiling during stone cell formation. *Mol. Biol. Rep.* **2019**, *46*, 2153–2175. [CrossRef]
75. Wei, Y.; Mu, H.; Xu, G.; Wang, Y.; Li, Y.; Li, S.; Wang, L. Genome-wide analysis and functional characterization of the UDP-glycosyltransferase family in grapes. *Horticulturae* **2021**, *7*, 204. [CrossRef]
76. Levasseur, A.; Pontarotti, P. The role of duplications in the evolution of genomes highlights the need for evolutionary-based approaches in comparative genomics. *Biol. Direct* **2011**, *6*, 11. [CrossRef]
77. Coen, O.; Magnani, E. Seed coat thickness in the evolution of angiosperms. *Cell. Mol. Life Sci.* **2018**, *75*, 2509–2518. [CrossRef]
78. Gardarin, A.; Durr, C.; Mannino, M.R.; Busset, H.; Colbach, N. Seed mortality in the soil is related to seed coat thickness. *Seed Sci. Res.* **2010**, *20*, 243–256. [CrossRef]
79. Kelly, K.M.; Vanstaden, J.; Bell, W.E. Seed coat structure and dormancy. *Plant Growth Regul.* **1992**, *11*, 201–209. [CrossRef]
80. Nooden, L.D.; Blakley, K.A.; Grzybowski, J.M. Control of seed coat thickness and permeability in soybean: A possible adaptation to stress. *Plant Physiol.* **1985**, *79*, 543–545. [CrossRef]
81. Mateo-Bonmati, E.; Casanova-Saez, R.; Simura, J.; Ljung, K. Broadening the roles of UDP-glycosyltransferases in auxin homeostasis and plant development. *New Phytol.* **2021**, *232*, 642–654. [CrossRef]
82. Baldacci-Cresp, F.; Le Roy, J.; Huss, B.; Lion, C.; Creach, A.; Spriet, C.; Duponchel, L.; Biot, C.; Baucher, M.; Hawkins, S.; et al. UDP-glycosyltransferase 72E3 plays a role in lignification of secondary cell walls in *Arabidopsis*. *Int. J. Mol. Sci.* **2020**, *21*, 6094. [CrossRef]
83. Aloni, R.; Tollier, M.T.; Monties, B. The role of auxin and gibberellin in controlling lignin formation in primary phloem fibers and in xylem of coleus blumei stems. *Plant Physiol.* **1990**, *94*, 1743–1747. [CrossRef] [PubMed]
84. Salazar, R.; Pollmann, S.; Morales-Quintana, L.; Herrera, R.; Caparros-Ruiz, D.; Ramos, P. In seedlings of Pinus radiata, jasmonic acid and auxin are differentially distributed on opposite sides of tilted stems affecting lignin monomer biosynthesis and composition. *Plant Physiol. Biochem.* **2019**, *135*, 215–223. [CrossRef] [PubMed]
85. Takeuchi, M.; Kegasa, T.; Watanabe, A.; Tamura, M.; Tsutsumi, Y. Expression analysis of transporter genes for screening candidate monolignol transporters using Arabidopsis thaliana cell suspensions during tracheary element differentiation. *J. Plant Res.* **2018**, *131*, 297–305. [CrossRef] [PubMed]
86. Fan, F.H.; Zhou, Z.J.; Qin, H.J.; Tan, J.H.; Ding, G.J. Exogenous brassinosteroid facilitates xylem development in pinus massoniana seedlings. *Int. J. Mol. Sci.* **2021**, *22*, 7615. [CrossRef]
87. Oh, M.H.; Honey, S.H.; Tax, F.E. The control of cell expansion, cell division, and vascular development by brassinosteroids: A historical perspective. *Int. J. Mol. Sci.* **2020**, *21*, 1743. [CrossRef]
88. Zhang, K.; Sun, Y.; Li, M.N.; Long, R.C. CrUGT87A1, a UDP-sugar glycosyltransferases (UGTs) gene from Carex rigescens, increases salt tolerance by accumulating flavonoids for antioxidation in *Arabidopsis thaliana*. *Plant Physiol. Biochem.* **2021**, *159*, 28–36. [CrossRef]
89. Wu, B.P.; Cao, X.M.; Liu, H.R.; Zhu, C.Q.; Klee, H.; Zhang, B.; Chen, K.S. UDP-glucosyltransferase PpUGT85A2 controls volatile glycosylation in peach. *J. Exp. Bot.* **2019**, *70*, 925–936. [CrossRef]
90. Zheng, H.; Zhang, C.L.; Wang, Y.T.; Zhou, W.T.; Chen, J.; Yan, X.Y.; Li, Z.Q.; Huang, S.Y.; Li, M.Y.; Tang, Y.; et al. Overexpression of the glucosyltransferase gene BoaUGT74B1 enhances the accumulation of indole glucosinolates in Chinese kale. *Sci. Hortic.* **2021**, *288*, 110302. [CrossRef]